



THIS MANUSCRIPT HAS BEEN SUBMITTED TO THE JOURNAL OF GLACIOLOGY AND HAS NOT BEEN PEER-REVIEWED.

Evidence that seismic anisotropy captures upstream palaeo ice fabric, with implications on present day deformation at Whillans Ice Stream, Antarctica

Journal:	<i>Journal of Glaciology</i>
Manuscript ID	Draft
Manuscript Type:	Article
Date Submitted by the Author:	n/a
Complete List of Authors:	Leung, Justin; Oxford University, Department of Earth Sciences Hudson, Thomas; Oxford University, Department of Earth Sciences Kendall, John-Michael; Oxford University, Department of Earth Sciences Barcheck, Grace; Cornell University, Department of Earth and Atmospheric Sciences
Keywords:	Ice streams, Seismology, Anisotropic ice
Abstract:	Understanding deformation and slip at ice streams, which are responsible for 90% of Antarctic ice loss, is vital for accurately modelling large-scale ice flow. Ice preferred crystal orientation fabric (COF) has a first-order effect on ice stream deformation. For the first time, we use shear-wave splitting (SWS) measurements of basal icequakes at Whillans Ice Stream (WIS), Antarctica, to determine a shear-wave anisotropy with an average delay time of 7 ms and fast S-wave polarisation (ϕ) of 29.3°. ϕ is expected to align perpendicular to ice flow, whereas our observation is oblique to the current ice flow direction ($\sim 280^\circ$). Our results suggest that ice at WIS preserves upstream fabric caused by palaeo-deformation developed over at least the past 450 years, implying that changes in the shape of WIS occurs on timescales shorter than COF re-equilibration. The "palaeo-fabric" can somewhat control present-day ice flow, which we suggest may somewhat counteract the long-term slowdown at WIS. Our findings suggest that seismic anisotropy can provide information on past ice sheet dynamics,

	and how past ice dynamics can play a role in controlling current deformation.

SCHOLARONE™
Manuscripts

Evidence that seismic anisotropy captures upstream palaeo ice fabric, with implications on present day deformation at Whillans Ice Stream, Antarctica

Justin LEUNG,¹ Thomas HUDSON,¹ John-Michael KENDALL,¹ Grace BARCHECK²

¹*Department of Earth Sciences, University of Oxford, Oxford, UK*

²*Department of Earth and Atmospheric Sciences, Cornell University, Ithaca, NY, USA*

Correspondence: Justin Leung <justin.leung@earth.ox.ac.uk>

ABSTRACT. Understanding deformation and slip at ice streams, which are responsible for 90% of Antarctic ice loss, is vital for accurately modelling large-scale ice flow. Ice preferred crystal orientation fabric (COF) has a first-order effect on ice stream deformation. For the first time, we use shear-wave splitting (SWS) measurements of basal icequakes at Whillans Ice Stream (WIS), Antarctica, to determine a shear-wave anisotropy with an average delay time of 7 ms and fast S-wave polarisation (φ) of 29.3°. φ is expected to align perpendicular to ice flow, whereas our observation is oblique to the current ice flow direction ($\sim 280^\circ$). Our results suggest that ice at WIS preserves upstream fabric caused by palaeo-deformation developed over at least the past 450 years, implying that changes in the shape of WIS occurs on timescales shorter than COF re-equilibration. The “palaeo-fabric” can somewhat control present-day ice flow, which we suggest may somewhat counteract the long-term slowdown at WIS. Our findings suggest that seismic anisotropy can provide information on past ice sheet dynamics, and how past ice dynamics can play a role in controlling current deformation.

24 INTRODUCTION

25 Despite ice streams spanning only 10% of Antarctica's surface area, they are responsible for 90% of Antarctic
26 ice loss (Morgan and others, 1982). Therefore, studying ice stream rheology is important for understanding
27 Antarctica's contribution to sea-level rise. One source of uncertainty in ice stream dynamics is the effect
28 of ice fabrics on rheology, where ice with a crystal oriented fabric (COF) can be ten times weaker in shear
29 in a particular direction relative to isotropic ice (Lutz and others, 2020). Glacial ice is commonly formed
30 of anisotropic hexagonal ice crystals, such that the viscosity along the basal plane of ice (normal to c-axis)
31 is sixty times less than that perpendicular to it (Duval and others, 1983). Under stress, the c-axes in a
32 bulk polycrystalline ice mass can rotate to form an ice COF over timescales of hundreds of years, which
33 can change in response to the stress it encounters (Azuma, 1994). Hence, understanding ice COF provides
34 insight on past deformation history and how it might influence future ice flow.

35 Most ice COF measurements are taken from microstructural analyses of ice core samples. However,
36 these are usually measured from stable or slow-moving regions of ice sheets, and cannot provide much
37 information of the physical processes in fast-deforming regions (Fan and others, 2021; Llorens and others,
38 2021). In contrast, seismic anisotropy measurements can be used to deduce ice COF properties over large
39 areas in different ice settings, including ice streams (Smith and others, 2017). Therefore, seismic anisotropy
40 can provide insight in these key fast-flowing regions, which can inform models of ice-sheet dynamics.

41 Whillans Ice Stream (WIS) is a major ice stream in West Antarctica that flows into the Ross Sea
42 embayment (see Figure 1; Picotti and others, 2015). The downstream portion of WIS is known as Whillans
43 Ice Plain (WIP), and it flows at a speed of over 300 metres per year, with stable sliding of the ice stream
44 punctuated 1-2 times daily by sudden unstable sliding motion during 30-minute slip events that also produce
45 high frequency icequakes and tremor (Barcheck and others, 2018; Bindschadler and others, 2003; Winberry
46 and others, 2013). Long-term slowdown of the ice stream can be seen, with longer periods of quiescence
47 between slip events over time, suggesting possibility of future stagnation (Winberry and others, 2014).
48 WIS is an excellent area to study basal seismicity given that seismic and GNSS data have been collected
49 over last decade at numerous sites to study its stick-slip cycle (e.g. Barcheck and others, 2020; Pratt and
50 others, 2014; Walter and others, 2011, 2015; Winberry and others, 2009, 2011) and basal hydrologic cycle
51 (e.g. Fricker and Scambos, 2009; Siegfried and others, 2016).

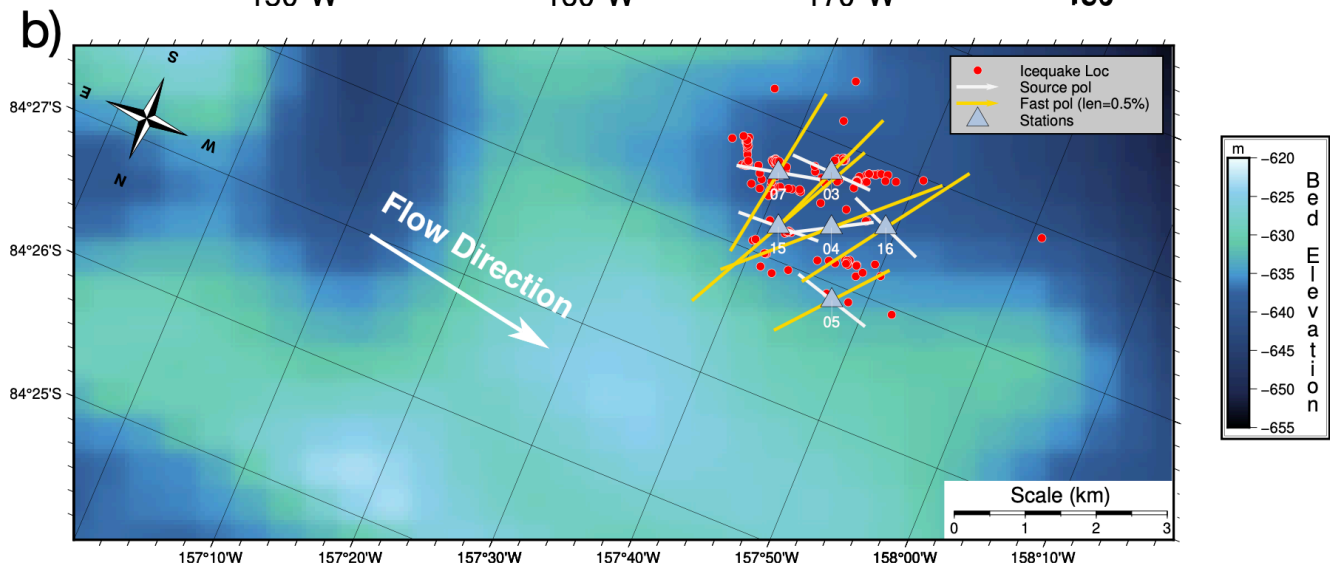
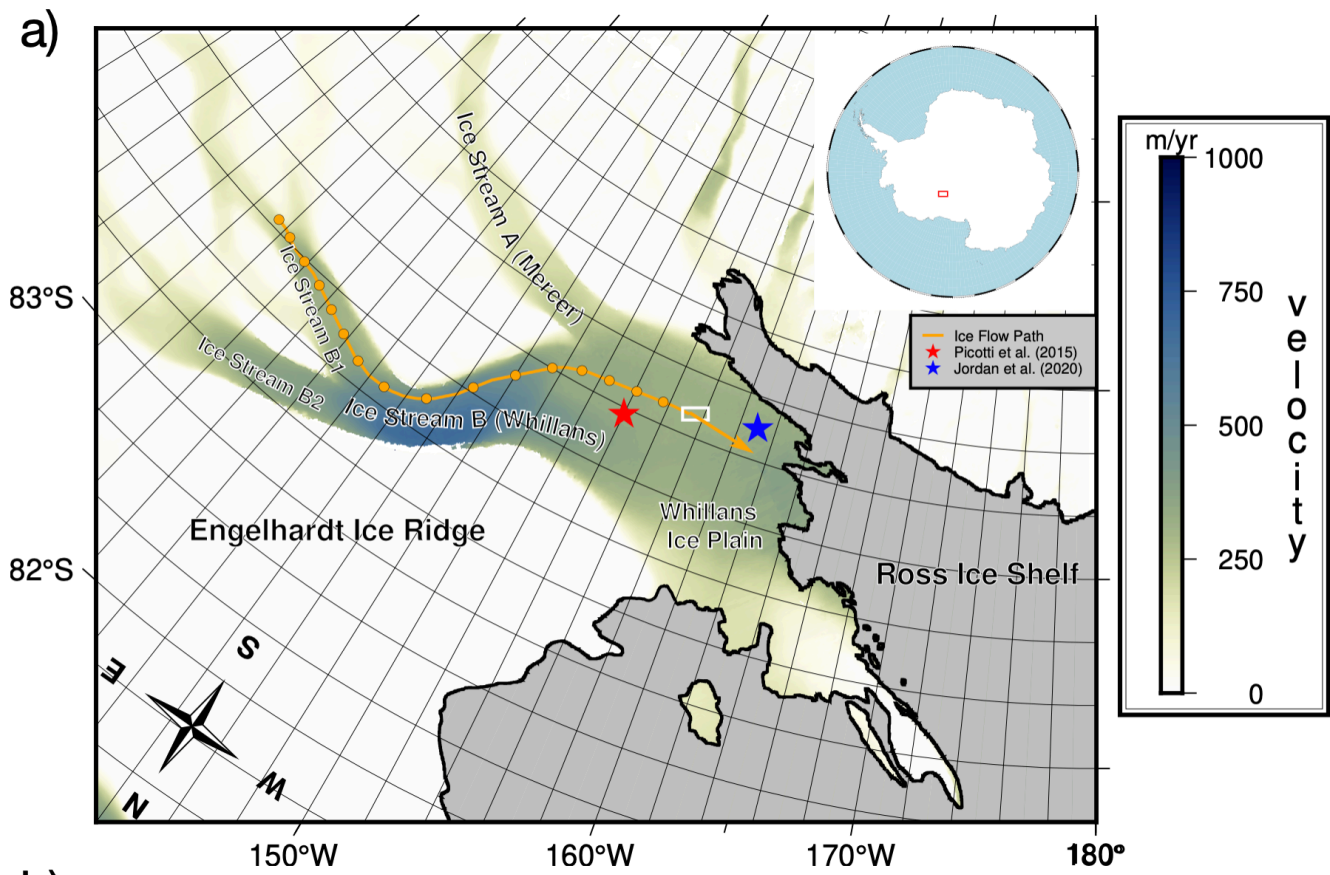


Fig. 1. Stereographic maps showing Whillans Ice Stream (WIS) and study location. (a) Regional map of the WIS. The grounding line is marked in the thick black line, and the grey shaded areas mark regions of floating ice. The blue and red star show the study site locations of Jordan and others (2020) and Picotti and others (2015) respectively. The orange line outlines the upstream flow path of the ice at our study site location, assuming current flow velocities, with orange points marking the locations at intervals of 50 years (see supplementary information for flow path calculation). The background colour map shows the ice flow velocity obtained from MEaSURES InSAR-Based Antarctica Ice Velocity Map, Version 2 (Rignot and others, 2017). The study area in (b) is outlined by the white box. (b) Detailed map of the study region. Stations are marked as blue triangles, and icequake locations are shown by red scatter points. Gold lines show the fast S-wave polarisation direction, with the length of the line representing the strength of anisotropy. White lines show the source polarisations for each event, as estimated from recorded shear waves. Dominant ice flow direction (280°) is indicated by the large white arrow. The background colour map shows the bed elevation Morlighem (2022).

There is currently an absence of ice COF observations for the entire ice column at WIS. Picotti and others (2015) used active seismic sources to suggest an azimuth-independent vertically transverse isotropic fabric (VTI) for the top 300 metres of WIS. Conversely, Jordan and others (2020) used electromagnetic methods to argue that the c-axes orient parallel to flow at WIS by polarimetric radar sounding that measured the top 400 metres of WIS (see Figure 1 for locations). Here, we provide the first seismic anisotropy measurements of the entire ice column at Whillans Ice Stream from shear-wave splitting of basal icequakes.

METHODOLOGY

This study uses 319 icequakes recorded between January 20th and February 27th, 2014 recorded by six seismometers at Whillans Ice Plain, Antarctica, part of a network active between 2012 to 2018 (Barcheck and others, 2020; Schwartz, 2012). The ice at the study site is between 690 and 710 m thick (Barcheck and others, 2020) and moving at ~370 m/a (Morlighem, 2022). Since horizontal orientation of the instruments is important for studying seismic anisotropy, we verified the orientation of these instruments using a teleseismic event. We performed a manual search for icequakes focused within the duration of bidaily slip events at WIS, which were initially detected by QuakeMigrate (Hudson and others, 2019) and described in Barcheck and others (2021). Icequake arrival times are picked manually and are located using NonLin-
Loc, a probabilistic non-linear earthquake location algorithm (Lomax and others, 2000). Only icequakes originating at the bed of the ice stream are of interest for measuring total anisotropy in the ice column,

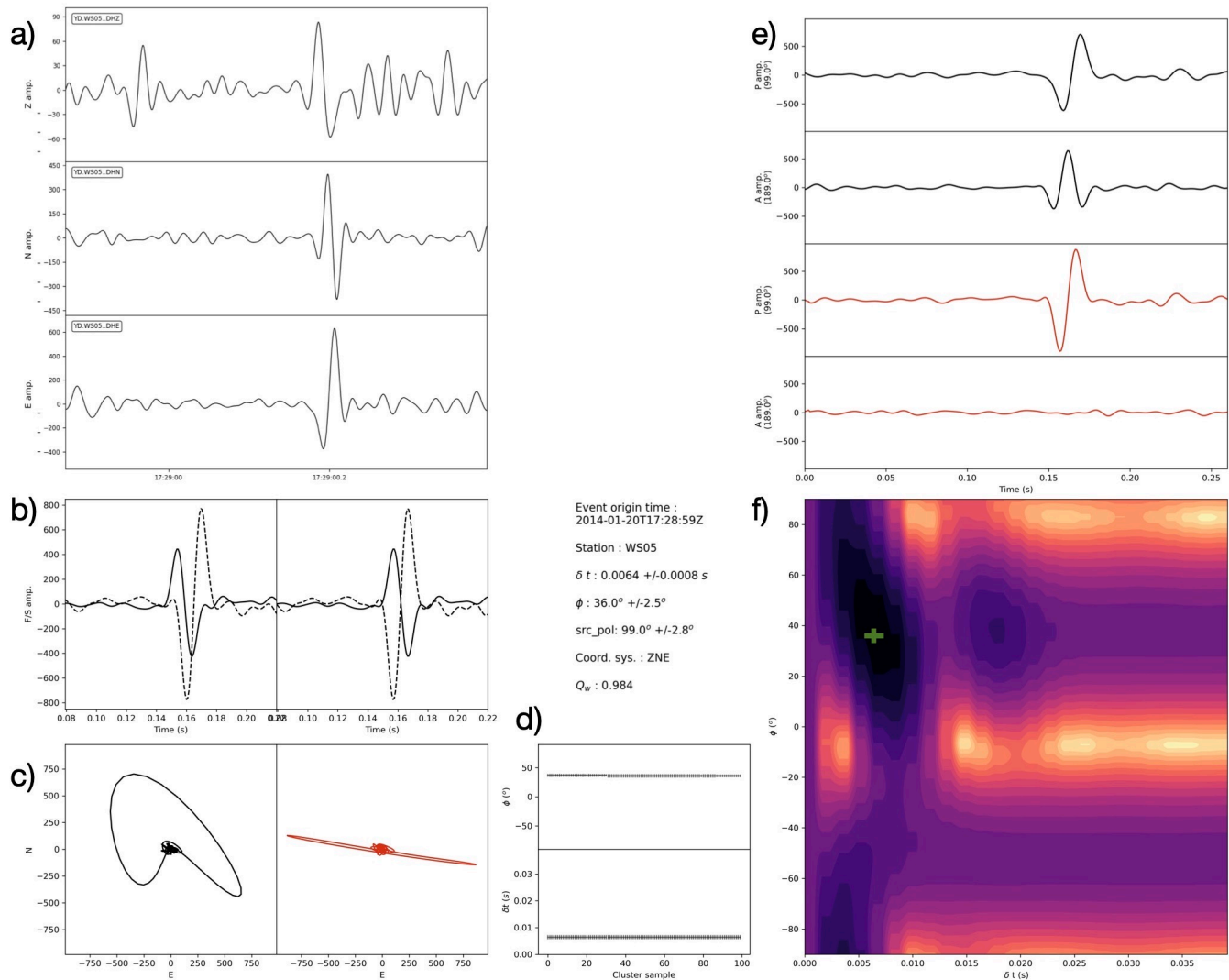


Fig. 2. An example of a well-constrained shear-wave splitting event. (a) Icequake signal before correction in the vertical, north and east component. (b) The waveforms before (left) and after (right) SWS correction, plotted in the fast (black line) and slow (dotted) directions. (c) Horizontal (north and east) particle motion before (left) and after (right) SWS correction (d) Optimal φ and δt for different cluster sizes. A good splitting measurement should have constant φ and δt values independent of cluster size. (e) Particle motion of icequakes in the source polarisation (P) and the perpendicular azimuth (A) before (top two) and after (bottom two) correction. (f) Error surface plotted on φ vs δt . Larger errors are represented with brighter colours, and smaller errors with darker colours. The optimal φ and δt and its uncertainties are shown with the green symbol.

72 therefore icequakes with a source depth shallower than 400 metres are removed. Each icequake is filtered
 73 by a 10-100 Hz bandpass filter, based on the dominant source spectra of the icequakes (see Figure S1).
 74 Seismic anisotropy is analysed on the horizontal (north and east) components because a ~100 m thick firn
 75 layer refracts the ray path of icequakes to near-vertical incidence at the surface (Picotti and others, 2015).

76 Shear-wave splitting (SWS) analysis is conducted using the python package SWSPy (Hudson and
 77 others, 2023a), based on the approach of Wuestefeld and others (2010). It can be summarised as follows:
 78 First, a range of analysis time windows are defined because SWS measurements are sensitive to window
 79 lengths (Teanby and others, 2004). Second, a grid search is performed over fast shear-wave polarisation
 80 of $-90^\circ < \varphi \leq 90^\circ$ and delay times between fast and slow S-waves of $0 \leq \delta t \leq 0.1$ for each window. The
 81 splitting parameters, φ and δt , associated with the minimum second eigenvalue of the S-wave covariance
 82 matrix that best linearize particle motion, describe the anisotropy observed along a given source-receiver
 83 ray path. Third, density-based cluster analysis is performed on all optimal φ and δt values, such that the
 84 optimal φ and δt values are obtained from the most stable cluster with minimum variance in φ and δt
 85 (Ester and others, 1996; Teanby and others, 2004). The source polarisation is then calculated by taking the
 86 azimuth of the largest eigenvalue of the covariance matrix of the linearised waveforms (Walsh and others,
 87 2013).

88 A well-constrained result after SWS correction is defined as satisfying the following four requirements:
 89 (1) the particle motion (see Figure 2c) becomes approximately linear after removing splitting using the
 90 optimal SWS parameters, (2) the error surface (see Figure 2f) has a unique, well-constrained solution, (3)
 91 splitting parameters (φ and δt) are stable (see Figure 2d) throughout different clusters, and (4) the quality
 92 factor Q_w is larger than 0.7. Q_w measures the robustness of the splitting measurement, and it is calculated
 93 by comparing the results from the eigenvalue method of Silver and Chan (1991) to the cross-correlation
 94 method of Menke and Levin (2003). A value of $Q_w = 1$ signifies a perfect match between the two methods,
 95 $Q_w = -1$ a good null result, and $Q_w = 0$ a poor result (Wuestefeld and others, 2010).

96 The strength of anisotropy (δV), or the difference between fast and slow S-wave velocities, can be
 97 quantified by the change in velocity, derived from the delay time (δt):

$$\delta V = (V \times \delta t \times 100)/r \quad (1)$$

98 where $V = 1944$ m/s is the average isotropic shear-wave speed (Smith and others, 2017) and r the
 99 source-receiver distance.

100 RESULTS

101 80 results from 70 events fulfil the aforementioned four criteria, and therefore are chosen for further analy-
102 sis. The fast S-wave polarisation φ and source polarisation of these events are plotted as polar histograms
103 in Figure 3. For a double-couple icequake source associated with ice slip at the bed, S-wave source po-
104 larisation is aligned with the direction of slip (Hudson and others, 2020). One might typically expect the
105 average S-wave source polarisation to align approximately with ice flow direction. Most source polarisation
106 measurements lie approximately in the east-west direction with an average of $264^\circ\text{N} \pm 22^\circ$, which is in
107 agreement with the Whillans Ice Stream's flow direction of $280^\circ\text{N} \pm 2^\circ$ (Rignot and others, 2017).

108 The average delay time for these results is 7.1 ms and ranges from 1.6 ms to 19.2 ms. The average
109 strength of anisotropy, δV , is $\sim 1.5\%$, with a maximum of 2.8%. This is below the maximum directional
110 variation in S-wave velocities of single ice crystals of 12% (Lutz and others, 2020).

111 The shear-wave splitting measurements have an overall mean fast S-wave direction (φ) of $29.3^\circ\text{N} \pm 18^\circ$
112 (see Figure 3a). The uncertainty in this result is defined as one standard deviation, likely representing an
113 upper estimate of uncertainty in the result that could be caused by temporal variations in φ (see Figure
114 S2). Individual receivers generally have mean φ that fall within a range of 22.4°N to 47.0°N (see Figure
115 1b), with the exception of station WS07, which has a mean φ of 9.1°N (see label 07, Figure 1b). Ice
116 core studies (Alley, 1988; Llorens and others, 2021) and seismic anisotropy studies (Kufner and others,
117 2023; Smith and others, 2017) have found that regions of longitudinal extension, such as ice divides and
118 ice streams, have a vertical girdle fabric. In such fabrics, φ is found to be perpendicular to the ice flow
119 direction (Harland and others, 2013). Based on ice flow direction derived from InSAR (Rignot and others,
120 2017) and the source polarisation data in Figure 3b, one would expect $\varphi \sim 10^\circ\text{N}$ at the Whillans study site
121 (golden arrow, Figure 3). However, the mean φ we observe of $29.3^\circ\text{N} \pm 18^\circ$ is oblique to this expected fast
122 S-wave direction of $\sim 10^\circ\text{N}$, even after accounting for uncertainty. A t-test shows that the 95% confidence
123 interval of the fast S-wave directions lies in between 25.3°N and 33.3°N (assuming that the distribution of
124 fast S-wave directions in the data is Gaussian), confirming our confidence in this obliquity.

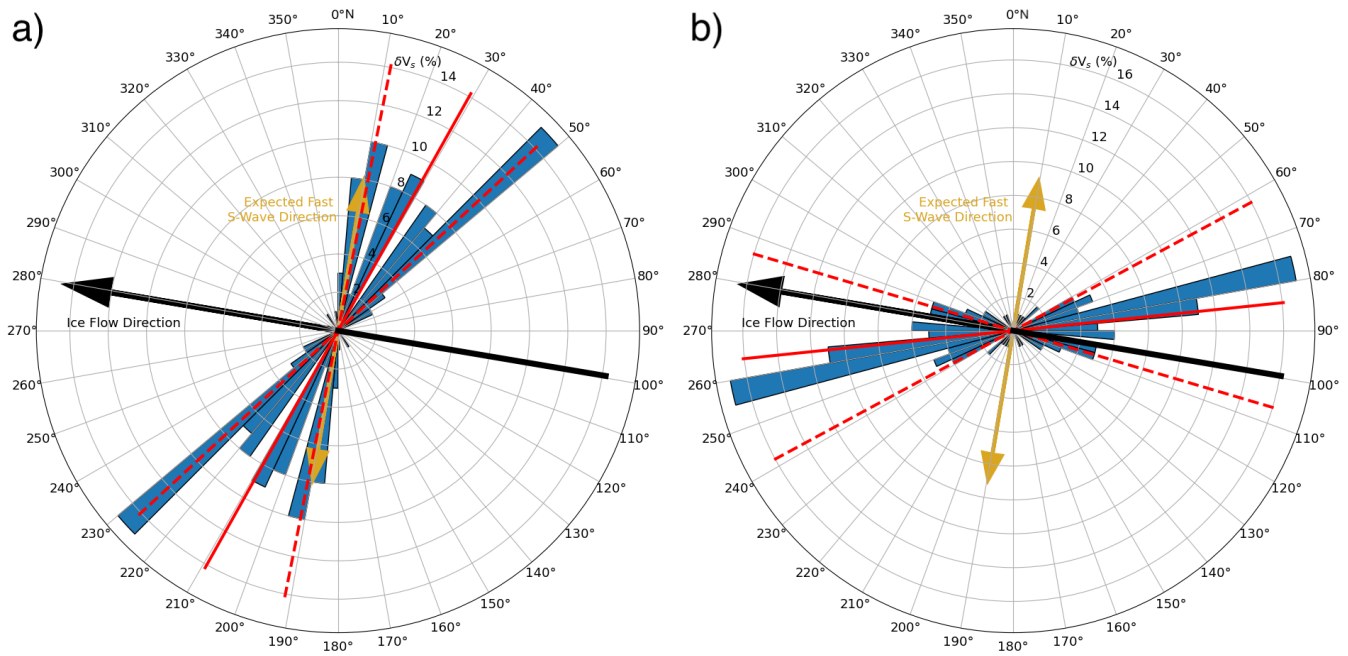


Fig. 3. Rose diagrams of (a) fast S-wave directions and (b) source polarisations for all the 80 SWS measurements. The solid and dotted red lines indicate the averages and uncertainties respectively. The gold arrows on both diagrams indicate the expected fast S-wave direction based on ice flow direction, which are shown as black arrows (see main text for further details). Method for estimating uncertainty is included in the supplementary information.

125 **DISCUSSION**126 **Possible origins of an ice COF with an oblique fast S-wave direction**

127 Our results suggest that the ice COF at Whillans Ice Stream (WIS) is oriented oblique, rather than
128 perpendicular, to the ice flow direction. This obliqueness suggests one of two hypotheses: either that the
129 local strain at our study site acts oblique to ice flow; or that the ice COF at WIS is the result of preservation
130 of historic deformation upstream of the study site.

131 Regarding the first hypothesis, a possible reason for extension oblique to ice flow is the differential ice
132 flux between the two tributaries of Whillans Ice Plain (WIP) across a suture zone. The study site is located
133 downstream of the confluence between the upper WIS and Mercer Ice Stream (MIS), where the faster flow
134 of WIS relative to MIS leads to shear strain across the suture zone, which can reorientate ice crystals (see
135 Figure 4; Beem and others, 2014). However, Bindschadler and others (1987) argue that shear is minimal
136 between WIS and MIS. Additionally, we postulate that this suture zone has a negligible effect on the ice
137 COF because the ice at our study site is in a laminar flow regime. Otherwise, we expect significant mixing
138 to occur between the two ice streams, which would perturb the ice fabric on length scales of the order of
139 hundreds of metres. This mixing would likely yield significant differences in the fast-polarisation S-wave
140 azimuth (φ) between the different stations, yet the fast-polarisation S-wave azimuths remain constant
141 within uncertainty across the network.

142 We instead favour the second hypothesis: that WIS has a “palaeo-COF” that preserves a record of
143 WIS’ upstream palaeo-deformation. Ice core studies suggest that such preservation of a COF upstream is
144 possible (Alley, 1988; Llorens and others, 2021). Additionally, most of the ice deformation at WIP occurs
145 along the shear margins (Truffer and Echelmeyer, 2003), so internal deformation at Whillans is minimal.
146 This minimal internal deformation would allow an upstream ice COF to be preserved at our study site,
147 and it implies that the main factor in ice fabric evolution at WIS is lattice rotation.

148 The ice COF always rotates towards the direction of most compression, which in ice streams is the
149 direction perpendicular to the flow direction (Smith and others, 2017; Thorsteinsson and others, 2003).
150 The meandering nature of WIS alters the direction of compression, and therefore the ice COF represents an
151 integrated history of upstream strain induced from this changing stress. As such, it is difficult to pinpoint
152 the origin of the fabric formation. However, for the ice COF to have developed the observed oblique φ , the
153 ice at our study site must have preserved some of its deformation history from when the flow direction was

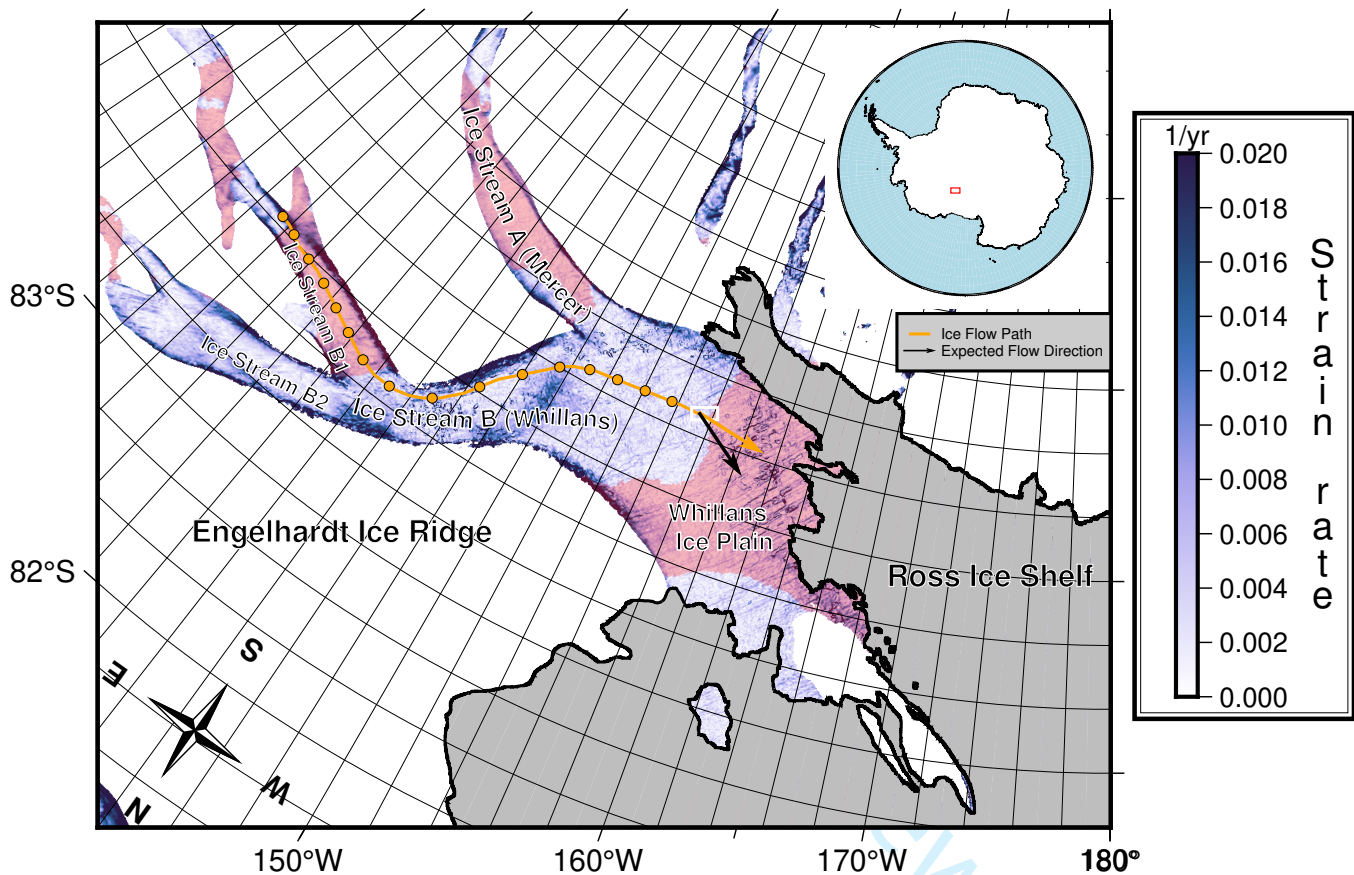


Fig. 4. A summary of the study findings. Regions with a flow direction between 281°N to 317°N , are shaded in red. The orange arrow shows the present-day flow direction, and the black arrow indicates the flow direction inferred from the fast S-wave polarisation direction. The background colour map is the strain rate calculated using Rignot and others (2017)'s velocity map (see supplementary information for calculation). Other features shown in this map are as in Figure 1a. The azimuth of the strain rate is shown in Figure S3.

perpendicular to φ . Considering the present-day westward flow direction only and fast S-wave polarisation uncertainties of 18° , these regions have a flow direction approximately in the west-northwest direction of 281°N to 317°N (see shaded red regions in Figure 4). The nearest region with such a flow direction along the ice flow path is in the southern tributary of WIS, indicating that the ice COF could not have been purely derived from the integrated strain alone over the past 450 years. Consequently, this implies that the flow direction of WIS changes on timescales shorter than ice COF re-equilibration. With this observation, we assume constant flow directions with time because ice-flow chronological studies do not suggest major changes in flow direction at WIS over the past 500 years (Catania and others, 2012). Furthermore, the validity of this assumption does not affect our conclusion of a palaeo-COF at WIS because present-day ice velocities are insufficient to explain the observed φ .

Larger strain rates can accelerate the rotation of lattices, and hence reduce the re-equilibration timescales of ice fabrics. From present-day velocities, the largest strain rates are located on the main trunk of WIS (see Figure 4). However, these strain rates could have been different in the past because of the dynamic nature of ice streams. Some studies show that ice streams in the Ross Sea sector have variable mass fluxes over the past centuries, in particular the Kamb Ice Stream (Bougamont and others, 2015; Catania and others, 2012; Conway and others, 2002). Further studies of ice anisotropy, in combination with more detailed past ice conditions and flow calculations, would further evidence any dynamic changes in ice anisotropy along WIS.

Given that the expected φ based on current ice flow is only just outside the uncertainty of our results, we cannot ignore the possibility of an ice COF derived from the present-day study site. However, there is only a negligible part of the study area that has a flow direction between 281°N and 317°N , with the remainder of this region located downstream of the study site (see red shaded regions in Figure 4). Hence, it is unlikely that enough time elapses for the ice COF to re-equilibrate with the present-day flow direction. We therefore suggest that the ice fabric is most likely derived from upstream palaeo-deformation.

Comparison to other COF studies at WIS

Our results of an oblique fast S-wave direction (φ) differ from both Picotti and others (2015)'s result of an azimuth-independent fabric and Jordan and others (2020)'s findings of φ parallel to flow. We attribute these differences to variations in sampling location and depth (see Figure 1a), with our study being the first to sample the effective anisotropy over the entire depth of WIS.

183 Jordan and others (2020) find a horizontal girdle fabric with φ parallel to flow, suggesting a longitudi-
184 nally compressive instead of longitudinally extensional stress regime. However, their study was conducted
185 near the grounding line (see Figure 1a), where stresses become longitudinally compressive due to stronger
186 interactions between the ice and the bed topography (Bindschadler and others, 1987; Picotti and others,
187 2015). Other studies suggest that the stress regime at WIP is longitudinally compressive (Bindschadler
188 and others, 1987). However, this likely does not apply to our study site. Firstly, the strain rates at WIS
189 vary massively as little as 20 kilometres (see Figure 9 of Bindschadler and others, 1987). Secondly, the ice
190 flow path inferred from present-day velocities indicates that the ice at our study site has travelled along
191 the outer part of the curve at WIP, where we expect the stress regime to be longitudinally extensional (see
192 Figure 4). Thirdly, longitudinal deviatoric stresses are also expected to be less prevalent farther away from
193 the grounding line (Picotti and others, 2015).

194 Picotti and others (2015) observe an azimuth-independent fabric, and suggest that ice streams with low
195 basal shear stress and highly-water-saturated sediments have COF profiles similar to ice divides due to the
196 increasing influence of vertical compression relative to transverse compression. Their study site is located
197 above Subglacial Lake Whillans, which is further inwards of the curve at WIP, where the stress regime
198 is less longitudinally extensional (see Figure 1a). Additionally, their ice COF is likely to have undergone
199 more equilibration caused by higher strain rates and lower flow velocities on the northern side of WIS (see
200 Figure 4; Bindschadler and others, 1987). Given this variance in ice COF in WIS, future studies of ice
201 deformation and anisotropy can furthermore reveal the spatial and temporal variability of ice COF at WIS.

202 **Comparison to other ice streams**

203 Shear-wave splitting studies from another Antarctic ice stream, Rutford Ice Stream (RIS), find that the
204 COF at RIS is approximately perpendicular ($\sim 85^\circ$) to ice flow (Harland and others, 2013; Smith and
205 others, 2017). Unlike the deviatoric nature of WIS stream flow, the flow direction at RIS is approximately
206 linear over COF re-equilibration timescales. As such, it is not possible to discriminate to what extent the
207 COF at RIS represents the current deformation or a preserved upstream deformation state. Kufner and
208 others (2023) suggest that the RIS COF signal is dominated by the latter.

209 The strength of anisotropy at RIS is 3-5%, while that at WIS is 1.5%. This difference can be attributed
210 to the driving stress, with the driving stress at RIS (40 kPa; Doake and others, 2001) at least twice that
211 at WIS (<20 kPa; Bentley, 1987). The two ice streams have similar flowing speeds, with RIS moving at

212 an average velocity of 377 m/a and WIS flowing at 370 m/a (Morlighem, 2022; Smith and others, 2017).
213 Hence, the difference in driving stress is accommodated by the difference in basal friction. This can be
214 explained by the relatively larger normal stress at RIS of 10 – 500 kPa, compared to that at WIS of 20 –
215 30 kPa (Hudson and others, 2023b; Lipovsky and Dunham, 2016). Lower friction at WIS results in less
216 internal deformation of the ice column, leading to lower strengths of anisotropy.

217 A recent seismic anisotropy study at RIS by Kufner and others (2023) suggested that multi-layer
218 anisotropy can be present in ice streams, where the deepest third of the ice stream is thought to comprise
219 an azimuthally isotropic cluster fabric caused by basal-shearing-induced dynamic recrystallisation (Azuma,
220 1994). However, the apparent absence of double arrival times combined with the minimal basal shear
221 stress at WIS (Bindschadler and others, 1987; Blankenship and others, 1986) suggest that any multi-layer
222 anisotropic effects at WIS are negligible.

223 **Implications of an oblique ice fabric on ice flow**

224 Ice with a COF with the c-axis of a girdle fabric oriented perpendicular to flow can flow up to ten times
225 faster than isotropic ice, because the viscosity of ice is sixty times lower parallel to the a-axis (the plane of
226 weakest viscosity in the anisotropic crystal structure) than the c-axis (Harland and others, 2013). However,
227 our results at WIS show a c-axis orientation that is not perpendicular, but oblique to ice flow. This implies
228 that WIS is not deforming internally at its fastest possible rate, slowed by the misalignment of the a-axis
229 with flow direction. This misalignment likely also contributes to the observation of little to no internal
230 deformation of Whillans Ice Plain (Truffer and Echelmeyer, 2003).

231 Our observations suggest that palaeo ice COF can somewhat control present-day ice flow. If the shape
232 of an ice stream deviates on length scales less than the distance ice travels within the COF re-equilibration
233 time, then the COF may not be aligned with ice flow, limiting the rate of deformation of the ice column
234 with respect to ice flow direction. If an ice stream flows linearly for a duration greater than the re-
235 equilibration time, then the COF should re-equilibrate with the bulk stress, such that the a-axis direction
236 will rotate parallel to the ice flow direction and increase the rate of deformation downstream. The degree
237 of re-equilibration of an ice COF with the surrounding stresses is not only dependent on ice stream shape,
238 but also on flow speed. Slower-flowing ice will have more time to re-equilibrate with the surrounding stress-
239 field. The long-term slowdown at WIS can therefore provide more time for its ice COF re-equilibration,
240 which in turn reduces the misalignment of the a-axis with flow direction and allows for faster flow. This

241 counteraction to the slowdown has consequences on future predictions of ice flow at WIS.

242 Most icesheet-scale ice dynamics models assume either that ice is isotropic, or parameterise anisotropy
243 effects via an enhancement factor to account for ice weakening due to COF orientation relative to ice
244 flow. However, recent studies such as Smith and others (2017) and Kufner and others (2023), suggest that
245 enhancement factors should no longer be used to parameterise ice viscosity in fast deforming regions such as
246 ice streams. Our findings at WIS further support the importance of characterising directionally-dependent
247 ice viscosity in ice flow models, and emphasise that understanding ice COF in both space and time is
248 important for producing more realistic deformation in ice dynamics models.

249 CONCLUSION

250 This study provides shear-wave splitting (SWS) observations from basal icequakes at Whillans Ice Stream
251 (WIS). From these observations, we infer the ice crystal orientation fabric (COF) anisotropy over the entire
252 ice column. The observations provide insight into past and present deformation at WIS. The results from
253 80 discrete icequakes SWS observations show that WIS has an average fast S-wave direction (φ) of 29.3° ,
254 which is oblique to the expected direction of $\sim 10^\circ$ based on ice flow direction at the study site of around
255 280° . We suggest that the ice COF records an integrated strain history along its flow path for at least the
256 past 450 years to have preserved deformation in the direction of φ . The non-perpendicularity of φ to ice
257 flow implies that the shape of an ice stream can affect its flow, such that spatially deviatoric ice streams
258 including WIS are not flowing at their fastest potential. Given the long-term slowdown of WIS, the a-axis
259 will have more time to re-equilibrate with the surrounding stress-field, which can counteract the long-term
260 slowdown. Our results have implications for ice sheet models, suggesting that historic ice flow can preserve
261 ice fabric and hence directionally-dependent ice viscosity that might play an important role in such models.

262 SUPPLEMENTARY MATERIAL

263 The supplementary material for this article can be found in `suppl_mat_WIS_anisotropy.pdf`, as attached
264 with the submission of this manuscript.

265 ACKNOWLEDGEMENTS

266 We thank Alex Brisbane for his comments, which have improved the manuscript.

267 **REFERENCES**

- 268 Alley RB (1988) Fabrics in Polar Ice Sheets: Development and Prediction. *Science*, **240**(4851), 493–495, ISSN
269 0036-8075, 1095-9203 (doi: 10.1126/science.240.4851.493)
- 270 Azuma N (1994) A flow law for anisotropic ice and its application to ice sheets. *Earth and Planetary Science Letters*,
271 **128**(3-4), 601–614, ISSN 0012821X (doi: 10.1016/0012-821X(94)90173-2)
- 272 Barcheck CG, Tulaczyk S, Schwartz SY, Walter JI and Winberry JP (2018) Implications of basal micro-earthquakes
273 and tremor for ice stream mechanics: Stick-slip basal sliding and till erosion. *Earth and Planetary Science Letters*,
274 **486**, 54–60, ISSN 0012821X (doi: 10.1016/j.epsl.2017.12.046)
- 275 Barcheck CG, Schwartz SY and Tulaczyk S (2020) Icequake streaks linked to potential mega-scale glacial lineations
276 beneath an Antarctic ice stream. *Geology*, **48**(2), 99–102, ISSN 0091-7613, 1943-2682 (doi: 10.1130/G46626.1)
- 277 Barcheck G, Brodsky EE, Fulton PM, King MA, Siegfried MR and Tulaczyk S (2021) Migratory earthquake precur-
278 sors are dominant on an ice stream fault. *Science Advances*, **7**(6), eabd0105, ISSN 2375-2548 (doi: 10.1126/sci-
279 adv.abd0105)
- 280 Beem LH, Tulaczyk SM, King MA, Bougamont M, Fricker HA and Christoffersen P (2014) Variable deceleration of
281 Whillans Ice Stream, West Antarctica. *Journal of Geophysical Research: Earth Surface*, **119**(2), 212–224, ISSN
282 21699003 (doi: 10.1002/2013JF002958)
- 283 Bentley CR (1987) Antarctic ice streams: A review. *Journal of Geophysical Research*, **92**(B9), 8843, ISSN 0148-0227
284 (doi: 10.1029/JB092iB09p08843)
- 285 Bindschadler RA, Stephenson SN, MacAyeal DR and Shabtaie S (1987) Ice dynamics at the mouth of ice stream B,
286 Antarctica. *Journal of Geophysical Research*, **92**(B9), 8885, ISSN 0148-0227 (doi: 10.1029/JB092iB09p08885)
- 287 Bindschadler RA, King MA, Alley RB, Anandakrishnan S and Padman L (2003) Tidally controlled stick-slip discharge
288 of a West Antarctic ice. *Science*, **301**(5636), 1087–1089
- 289 Blankenship DD, Bentley CR, Rooney ST and Alley RB (1986) Seismic measurements reveal a saturated porous
290 layer beneath an active Antarctic ice stream. *Nature*, **322**(6074), 54–57, ISSN 0028-0836, 1476-4687 (doi:
291 10.1038/322054a0)
- 292 Bougamont M, Christoffersen P, Price SF, Fricker HA, Tulaczyk S and Carter SP (2015) Reactivation of Kamb Ice
293 Stream tributaries triggers century-scale reorganization of Siple Coast ice flow in West Antarctica. *Geophysical
294 Research Letters*, **42**(20), 8471–8480, ISSN 0094-8276, 1944-8007 (doi: 10.1002/2015GL065782)

- 295 Catania G, Hulbe C, Conway H, Scambos T and Raymond C (2012) Variability in the mass flux of the Ross ice
296 streams, West Antarctica, over the last millennium. *Journal of Glaciology*, **58**(210), 741–752, ISSN 0022-1430,
297 1727-5652 (doi: 10.3189/2012JoG11J219)
- 298 Conway H, Catania G, Raymond CF, Gades AM, Scambos TA and Engelhardt H (2002) Switch of flow direction in
299 an Antarctic ice stream. *Nature*, **419**(6906), 465–467, ISSN 0028-0836, 1476-4687 (doi: 10.1038/nature01081)
- 300 Doake CSM, Corr HFJ, Jenkins A, Makinson K, Nicholls KW, Nath C, Smith AM and Vaughan DG (2001) Rut-
301 ford Ice Stream, Antarctica. In *The West Antarctic Ice Sheet: Behavior and Environment*, 221–235, Ameri-
302 can Geophysical Union (AGU), ISBN 978-1-118-66832-0 (doi: <https://doi.org/10.1029/AR077p0221>), _eprint:
303 <https://agupubs.onlinelibrary.wiley.com/doi/pdf/10.1029/AR077p0221>
- 304 Duval P, Ashby MF and Anderman I (1983) Rate-controlling processes in the creep of polycrystalline ice. *The Journal*
305 *of Physical Chemistry*, **87**(21), 4066–4074, ISSN 0022-3654, 1541-5740 (doi: 10.1021/j100244a014)
- 306 Ester M, Kriegel HP and Xu X (1996) A Density-Based Algorithm for Discovering Clusters in Large Spatial Databases
307 with Noise
- 308 Fan S, Cross AJ, Prior DJ, Goldsby DL, Hager TF, Negrini M and Qi C (2021) Crystallographic Preferred Ori-
309 entation (CPO) Development Governs Strain Weakening in Ice: Insights From High-Temperature Deformation
310 Experiments. *Journal of Geophysical Research: Solid Earth*, **126**(12), e2021JB023173, ISSN 2169-9313, 2169-9356
311 (doi: 10.1029/2021JB023173)
- 312 Fricker HA and Scambos T (2009) Connected subglacial lake activity on lower Mercer and Whillans Ice
313 Streams, West Antarctica, 2003–2008. *Journal of Glaciology*, **55**(190), 303–315, ISSN 0022-1430, 1727-5652 (doi:
314 10.3189/002214309788608813)
- 315 Harland S, Kendall JM, Stuart G, Lloyd G, Baird A, Smith A, Pritchard H and Brisbourne A (2013) Deformation
316 in Rutford Ice Stream, West Antarctica: measuring shear-wave anisotropy from icequakes. *Annals of Glaciology*,
317 **54**(64), 105–114, ISSN 0260-3055, 1727-5644 (doi: 10.3189/2013AoG64A033)
- 318 Hudson T, Asplet J and Walker A (2023a) Automated shear-wave splitting analysis for single- and multi- layer
319 anisotropic media. preprint, Earth Sciences (doi: 10.31223/X5R67Z)
- 320 Hudson TS, Smith J, Brisbourne AM and White RS (2019) Automated detection of basal icequakes and dis-
321 crimination from surface crevassing. *Annals of Glaciology*, **60**(79), 167–181, ISSN 0260-3055, 1727-5644 (doi:
322 10.1017/aog.2019.18)
- 323 Hudson TS, Brisbourne AM, Walter F, Gräff D, White RS and Smith AM (2020) Icequake Source Mechanisms
324 for Studying Glacial Sliding. *Journal of Geophysical Research: Earth Surface*, **125**(11), e2020JF005627, ISSN
325 2169-9003, 2169-9011 (doi: 10.1029/2020JF005627)

- 326 Hudson TS, Kufner SK, Brisbourne AM, Kendall JM, Smith AM, Alley RB, Arthern RJ and Murray T (2023b)
327 Highly variable friction and slip observed at Antarctic ice stream bed. *Nature Geoscience*, **16**(7), 612–618, ISSN
328 1752-0894, 1752-0908 (doi: 10.1038/s41561-023-01204-4)
- 329 Jordan TM, Schroeder DM, Elsworth CW and Siegfried MR (2020) Estimation of ice fabric within Whillans Ice
330 Stream using polarimetric phase-sensitive radar sounding. *Annals of Glaciology*, **61**(81), 74–83, ISSN 0260-3055,
331 1727-5644 (doi: 10.1017/aog.2020.6)
- 332 Kufner S, Wookey J, Brisbourne AM, Martín C, Hudson TS, Kendall JM and Smith AM (2023) Strongly
333 Depth-Dependent Ice Fabric in a Fast-Flowing Antarctic Ice Stream Revealed With Icequake Observations.
334 *Journal of Geophysical Research: Earth Surface*, **128**(3), e2022JF006853, ISSN 2169-9003, 2169-9011 (doi:
335 10.1029/2022JF006853)
- 336 Lipovsky BP and Dunham EM (2016) Tremor during ice-stream stick slip. *The Cryosphere*, **10**(1), 385–399, ISSN
337 1994-0424 (doi: 10.5194/tc-10-385-2016)
- 338 Llorens MG, Griera A, Bons PD, Weikusat I, Prior D, Gomez-Rivas E, De Riese T, Jimenez-Munt I, García Castel-
339 lanos D and Lebensohn RA (2021) Can changes in ice-sheet flow be inferred from crystallographic preferred
340 orientations? preprint, Ice sheets/Numerical Modelling (doi: 10.5194/tc-2021-224)
- 341 Lomax A, Virieux J, Volant P and Berge-Thierry C (2000) Probabilistic Earthquake Location in 3D and Layered
342 Models. In CH Thurber and N Rabinowitz (eds.), *Advances in Seismic Event Location*, 101–134, Springer Nether-
343 lands, Dordrecht, ISBN 978-94-015-9536-0 (doi: 10.1007/978-94-015-9536-0_5)
- 344 Lutz F, Eccles J, Prior DJ, Craw L, Fan S, Hulbe C, Forbes M, Still H, Pyne A and Mandeno D (2020) Con-
345 straining Ice Shelf Anisotropy Using Shear Wave Splitting Measurements from Active-Source Borehole Seis-
346 mics. *Journal of Geophysical Research: Earth Surface*, **125**(9), e2020JF005707, ISSN 2169-9003, 2169-9011 (doi:
347 10.1029/2020JF005707)
- 348 Menke W and Levin V (2003) The cross-convolution method for interpreting *SKS* splitting observations, with appli-
349 cation to one and two-layer anisotropic earth models. *Geophysical Journal International*, **154**(2), 379–392, ISSN
350 0956540X, 1365246X (doi: 10.1046/j.1365-246X.2003.01937.x)
- 351 Morgan V, Jacka T, Akerman G and Clarke A (1982) Outlet Glacier and Mass-Budget Studies in Enderby, Kemp,
352 and Mac. Robertson Lands, Antarctica. *Annals of Glaciology*, **3**, 204–210, ISSN 0260-3055, 1727-5644 (doi:
353 10.3189/S0260305500002780)
- 354 Morlighem M (2022) MEaSURES BedMachine Antarctica, Version 3 (doi: 10.5067/FPSU0V1MWUB6)

- 355 Picotti S, Vuan A, Carcione JM, Horgan HJ and Anandakrishnan S (2015) Anisotropy and crystalline fabric of
356 Whillans Ice Stream (West Antarctica) inferred from multicomponent seismic data. *Journal of Geophysical Re-*
357 *search: Solid Earth*, **120**(6), 4237–4262, ISSN 2169-9313, 2169-9356 (doi: 10.1002/2014JB011591)
- 358 Pratt MJ, Winberry JP, Wiens DA, Anandakrishnan S and Alley RB (2014) Seismic and geodetic evidence for
359 grounding-line control of Whillans Ice Stream stick-slip events: Whillans Ice Stream Stick-Slip Events. *Journal of*
360 *Geophysical Research: Earth Surface*, **119**(2), 333–348, ISSN 21699003 (doi: 10.1002/2013JF002842)
- 361 Rignot E, Mouginit J, Morlighem M and Scheuchl B (2017) MEaSURES InSAR-Based Antarctica Ice Velocity Map,
362 Version 2 (doi: 10.5067/D7GK8F5J8M8R)
- 363 Schwartz SY (2012) Whillans Ice Stream Subglacial Access Research Drilling (doi: 10.7914/SN/YD_2012)
- 364 Siegfried MR, Fricker HA, Carter SP and Tulaczyk S (2016) Episodic ice velocity fluctuations triggered by a sub-
365 glacial flood in West Antarctica. *Geophysical Research Letters*, **43**(6), 2640–2648, ISSN 0094-8276, 1944-8007 (doi:
366 10.1002/2016GL067758)
- 367 Smith EC, Baird AF, Kendall JM, Martín C, White RS, Brisbourne AM and Smith AM (2017) Ice fabric in an
368 Antarctic ice stream interpreted from seismic anisotropy. *Geophysical Research Letters*, **44**(8), 3710–3718, ISSN
369 0094-8276, 1944-8007 (doi: 10.1002/2016GL072093)
- 370 Teanby NA, Kenda NA, Kendall JM, Martin C, White RS, Brisbourne AM and Smith AM (2004) Automation
371 of Shear-Wave Splitting Measurements using Cluster Analysis. *Bulletin of the Seismological Society of America*,
372 **94**(2), 453–463, ISSN 0037-1106 (doi: 10.1785/0120030123)
- 373 Thorsteinsson T, Waddington ED and Fletcher RC (2003) Spatial and temporal scales of anisotropic effects in
374 ice-sheet flow. *Annals of Glaciology*, **37**, 40–48, ISSN 0260-3055, 1727-5644 (doi: 10.3189/172756403781815429)
- 375 Truffer M and Echelmeyer KA (2003) Of isbræ and ice streams. *Annals of Glaciology*, **36**, 66–72, ISSN 0260-3055,
376 1727-5644 (doi: 10.3189/172756403781816347)
- 377 Walsh E, Arnold R and Savage MK (2013) Silver and Chan revisited: SILVER AND CHAN REVISITED. *Journal*
378 *of Geophysical Research: Solid Earth*, **118**(10), 5500–5515, ISSN 21699313 (doi: 10.1002/jgrb.50386)
- 379 Walter JI, Brodsky EE, Tulaczyk S, Schwartz SY and Pettersson R (2011) Transient slip events from near-field
380 seismic and geodetic data on a glacier fault, Whillans Ice Plain, West Antarctica: RUPTURE SPEEDS ON
381 WHILLANS ICE PLAIN. *Journal of Geophysical Research: Earth Surface*, **116**(F1), n/a–n/a, ISSN 01480227
382 (doi: 10.1029/2010JF001754)

- 383 Walter JI, Svetlizky I, Fineberg J, Brodsky EE, Tulaczyk S, Grace Barcheck C and Carter SP (2015) Rupture speed
384 dependence on initial stress profiles: Insights from glacier and laboratory stick-slip. *Earth and Planetary Science*
385 *Letters*, **411**, 112–120, ISSN 0012821X (doi: 10.1016/j.epsl.2014.11.025)
- 386 Winberry JP, Anandakrishnan S, Alley RB, Bindschadler RA and King MA (2009) Basal mechanics of ice streams:
387 Insights from the stick-slip motion of Whillans Ice Stream, West Antarctica. *Journal of Geophysical Research*,
388 **114**(F1), F01016, ISSN 0148-0227 (doi: 10.1029/2008JF001035)
- 389 Winberry JP, Anandakrishnan S, Wiens DA, Alley RB and Christianson K (2011) Dynamics of stick–slip motion,
390 Whillans Ice Stream, Antarctica. *Earth and Planetary Science Letters*, **305**(3-4), 283–289, ISSN 0012821X (doi:
391 10.1016/j.epsl.2011.02.052)
- 392 Winberry JP, Anandakrishnan S, Wiens DA and Alley RB (2013) Nucleation and seismic tremor associated with
393 the glacial earthquakes of Whillans Ice Stream, Antarctica. *Geophysical Research Letters*, **40**(2), 312–315, ISSN
394 0094-8276, 1944-8007 (doi: 10.1002/grl.50130)
- 395 Winberry JP, Anandakrishnan S, Alley RB, Wiens DA and Pratt MJ (2014) Tidal pacing, skipped slips and the
396 slowdown of Whillans Ice Stream, Antarctica. *Journal of Glaciology*, **60**(222), 795–807, ISSN 0022-1430, 1727-5652
397 (doi: 10.3189/2014JoG14J038)
- 398 Wuestefeld A, Al-Harrasi O, Verdon JP, Wookey J and Kendall JM (2010) A strategy for automated analysis of
399 passive microseismic data to image seismic anisotropy and fracture characteristics: A strategy for automated anal-
400 ysis of passive microseismic data. *Geophysical Prospecting*, **58**(5), 755–773, ISSN 00168025 (doi: 10.1111/j.1365-
401 2478.2010.00891.x)